Journal of Geodesy (1998) 72: 617–625

Journal of Geodesy

Calibration of satellite gradiometer data aided by ground gravity data

D. Arabelos[1], C. C. Tscherning[2]

[1] Department of Geodesy and Surveying, University of Thessaloniki, GR-540 06 Thessaloniki, Greece e-mail: arab@eng.auth.gr; Tel: +30 31 996091; Fax: +30 31 996408
[2] Department of Geophysics, University of Copenhagen, Juliane Maries Vej 30, DK-2100 Copenhagen, Denmark

Received: 10 October 1996 / Accepted 25 May 1998

Abstract. Parametric least squares collocation was used in order to study the detection of systematic errors of satellite gradiometer data. For this purpose, simulated data sets with a priori known systematic errors were produced using ground gravity data in the very smooth gravity field of the Canadian plains. Experiments carried out at different satellite altitudes showed that the recovery of bias parameters from the gradiometer "measurements" is possible with high accuracy, especially in the case of crossing tracks. The mean value of the differences (original minus estimated bias parameters) was relatively large compared to the standard deviation of the corresponding second-order derivative component at the corresponding height. This mean value almost vanished when gravity data at ground level were combined with the second-order derivative data set at satellite altitude. In the case of simultaneous estimation of bias and tilt parameters from $\partial^2 T/\partial z^2$ "measurements", the recovery of both parameters agreed very well with the collocation error estimation.

Key words. Satellite gradiometer data · Parametric collocation

1 Introduction

A spaceborne gravity mission will be executed using Satellite to Satellite Tracking (SST) and/or Satellite Gravity Gradiometry (SGG). In both cases the quality of the result must be assessed in an independent manner. As a supplement to on-board calibration and monitoring, the occurrence of systematic errors must be modelled, detected and eliminated if present.

Correspondence to: D. Arabelos

Already, the way the measurements are collected may aid in this task, i.e. we may use the fact that the ground tracks of the orbits cross each other, hereby making it possible to take advantage of the strong spatial correlation of the satellite data. We have studied how this may aid in detecting systematic errors (biases and tilts).

A similar strong correlation is obviously present between space data and ground data – otherwise we could not aim at using space data for determining geoid and gravity at ground level. We may take advantage of this and use data in areas with very well determined gravity anomalies. Using simulated data from an area with very smooth gravity anomalies, we have shown how systematic errors may be determined and eliminated. The advantage of using an area with smooth gravity is that we obtain a very good signal-to-noise ratio, which helps experiments with random and systematic errors.

The smooth area studied is located on the Canadian plains ($56° \leq \phi \leq 68°, -126° \leq \lambda \leq -106°$). Inside this area is an even smoother area ($59.5° \leq \phi \leq 64.5°, -117.5° \leq \lambda \leq -112.5°$) with gravity standard deviation (SD) (after subtraction of a high order reference field) of only 7 mGal. Gravity and gravity gradient values were computed at altitude using Least Squares Collocation (LSC), and also the Poisson integral implemented using the Fast Fourier Transform (FFT) technique (Schwarz et al. 1990), as a consistency check.

Since it is still uncertain at which altitude a satellite mission will be carried out, the quantities were computed at three different satellite altitudes: 200, 300 and 400 km, which covers the altitude range discussed at present.

Adding biases and tilts to these data, new data sets were produced. These data sets were used as simulated satellite data. The method of LSC (Moritz 1980) was used in order to study the possibility of recovering the a priori known systematic errors of the simulated satellite gradiometer data.

For the second-order derivatives of the anomalous potential T with respect to a local (x, y, z) coordinate frame (East, North, Up), we use the following notation:

$$\frac{\partial^2 T}{\partial x^2} = T_{xx}, \quad \frac{\partial^2 T}{\partial y^2} = T_{yy}, \quad \frac{\partial^2 T}{\partial z^2} = T_{zz}, \quad \frac{\partial^2 T}{\partial x \partial y} = T_{xy},$$
$$\frac{\partial^2 T}{\partial x \partial y} = T_{xz}, \quad \frac{\partial^2 T}{\partial y \partial z} = T_{yz}$$

2 Ground data collection

Ground data may be used for two purposes. One purpose is the use of the data in combination with satellite data. Another is the use of the data for the calibration of the satellite data, i.e. the assessment of the result of downward continued values or the detection of possible systematic errors in the space data. It is the latter application which we will describe here.

The gravity data set used in the present study was made available to the authors by R Forsberg (pers. comm). This data set includes 14,177 point free-air gravity anomalies in the area bounded by ($56° \leq \phi \leq 68°$, $-126° \leq \lambda \leq -106°$).

The distribution of the data is shown in Fig. 1. As it is seen from Fig. 1, the distribution of the data is very dense except in the area close to the meridian of $-124°$and in the regions of several lakes. The statistics of the point gravity values are shown in Table 1. In Fig. 2 the corresponding free-air gravity field after removal of the OSU91A (Rapp and Pavlis, 1990) contribution is shown. From Fig. 2, as well as from the statistics of Table 1, it is clear that the reduced free-air gravity anomaly field is very smooth, especially in the centre of the test area.

Omitting the data west of the meridian of $-124°$, the free-air gravity anomalies (after the removal of the OSU91A contribution) covering the area ($56° \leq \phi \leq 68°$, $-124° \leq \lambda \leq -106°$), in future called area A, were used for the creation of simulated space data sets as described in Sect. 3.

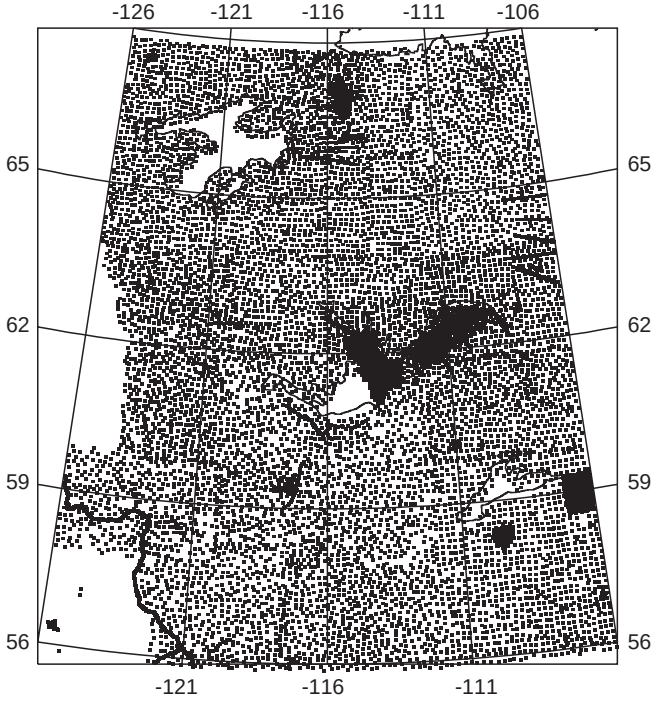

Fig. 1. Distribution of point gravity data

Table 1. Statistics of the free-air gravity anomalies in Canada (mGal)

	No.	Mean	SD	Min	Max
Original	14,177	−10.77	22.42	−81.10	133.00
Original − OSU91A	14,177	0.95	12.68	−159.06	148.10
Original − OSU91A[a]	13,339	1.21	10.89	−42.80	73.05

[a]After omitting the data to the west of the meridian of $-124°$ where the data coverage is poor.

3 Creation of simulated space data in the test area at different altitudes

The LSC method as implemented in the program GEOCOL (Tscherning 1995) was used to predict satellite data from ground data at different altitudes. This is done by multiplying covariances between the ground and the space data with weights obtained by solving a system of equations with a dimension equal to the number of ground data used. If data are clustered, singularities may occur in the case of points having almost identical coordinates. In order to avoid this problem a new data set was created by selecting data closest to the nodes of a $3' \times 3'$ grid. The equidistance of this grid corresponds to the mean distance between the original data.

The covariances of the ground data are estimated by forming products between all data and grouping the data in bins according to the distance. In order to reduce this task, data point values were selected closest to the nodes of a $10' \times 10'$ grid. In this way the empirical covariance function was computed from 6324 point values. The computed empirical covariance function has a correlation length equal to about 6.5′. The empirical covariance function was fitted with an analytic expression (model) using the program COVFIT (Knudsen 1987). Using the model parameters the auto- and cross-covariance function of any other kind of quantities related to the gravity field can be analytically computed, at any altitude. The empirical and the estimated analytical covariance functions of free-air gravity anomalies are shown in Fig. 3. The analytically derived values of standard deviations for various quantities related to the gravity field at three different altitudes are shown in Table 2.

The correlation length of the cross-covariance functions between gravity anomalies and second-order derivatives is considerably larger than the corresponding one of the auto-covariance function of gravity anomalies at ground level. Moreover, this correlation length increases with altitude. In Fig. 4 the cross-covariance function between gravity anomalies and T_{zz} is shown for

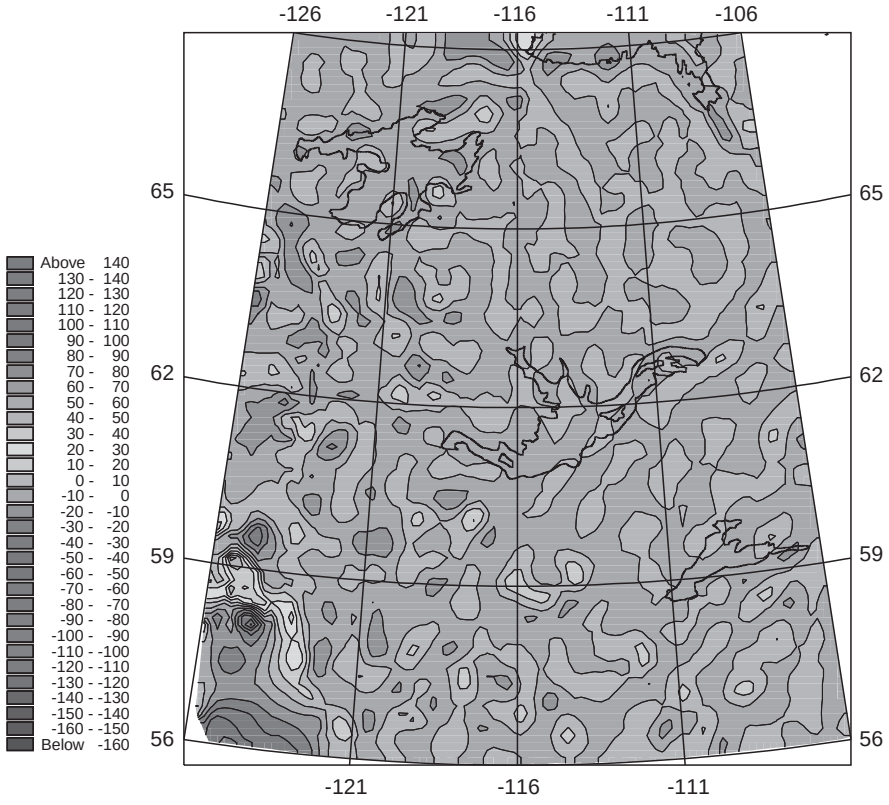

Fig. 2. The free-air gravity anomalies after removal of OSU91A contribution

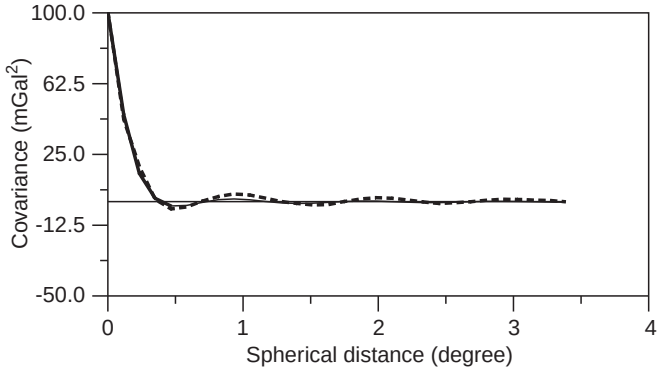

Fig. 3. Covariance function of the free-air gravity anomalies reduced to OSU91A in Canada (data set A). *Dashed line* Empirical; *solid line* analytical

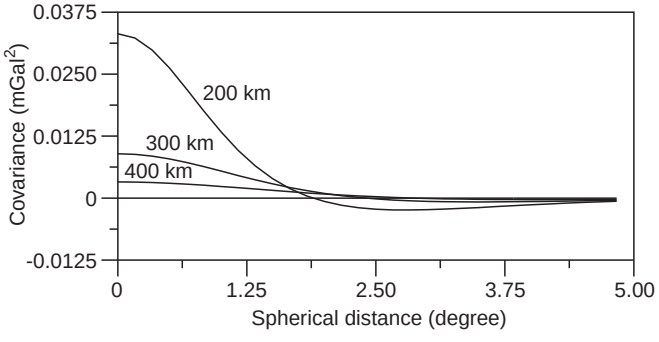

Fig. 4. Cross-covariance function between free-air gravity anomalies at ground level and *Tzz* at three different altitudes (200, 300 and 400 km)

Table 2. Analytically derived standard deviations of gravity and of three different types of second-order derivatives (for four different altitudes related to area A)

Altitude (km)	Gravity (mGal)	T_{zz} (EU)	$2*T_{xy}$ (EU)	T_{xx} (EU)
0	10.027	21.005	14.849	12.849
200	0.200	0.017	0.012	0.010
300	0.104	0.007	0.004	0.004
400	0.062	0.003	0.003	0.0001

three different altitudes. Due to this correlation length, for the prediction of second-order derivatives in a test area, gravity anomalies in a considerably larger area should be taken into account. For this reason, and in order to reduce the number of input data in the collocation experiments, a $30' \times 30'$ data set of gravity anomalies was computed by averaging the point values. This data set was used as input in the LSC upward continuation experiments for the computation of gravity gradients at three different satellite altitudes: 200, 300 and 400 km. Using LSC we computed T_{zz}, T_{xx}, T_{yy}, T_{xz}, T_{yz} and T_{xy} on a 15×15 ft. grid in the area bounded by $(59.5^\circ \leq \phi \leq 64.5^\circ, -117.5^\circ \leq \lambda \leq -112.5^\circ)$.

The equidistance of the grid was chosen to agree with the expected resolution of the satellite gravity gradiometer measurements. In this way, 3×6 new files were created with the simulated gradients (21×21 values per file) at the three different satellite altitudes. Simultaneously, the prediction (upward continuation) error was

computed. In the following this data set will be called data set A.

Slightly better results in terms of the signal-to-noise ratio were obtained using a "more local" covariance function, i.e. a covariance function computed using only the data included in the point data selection area ($59.5° \leq \phi \leq 64.5°, -117.5° \leq \lambda \leq -112.5°$). This inner area, in future called area B, is smoother than the entire area, having a variance of the gravity anomalies equal to 52 mGal^2 (see Fig. 5). The standard deviations for various quantities according to this "local" covariance function are given in Table 3. In future on this data set will be called data set B.

The real satellite measurements are actually high- and low-pass filtered values along track. This means that spectral features above and below a certain frequency are not included in their spectrum. In order to simulate such measurements we have to filter out the high- and the low-frequency information. One way to do the first is to substitute the point values by mean values along track with the same sampling as the real measurements. The filtering of the lower frequencies has been simulated by subtracting a high-order field (OSU91A). If the calculations are to be carried out for a specific instrument, the appropriate filter characteristics should obviously be used.

With the following experiment we tried to investigate whether the high-order frequencies would cause a problem, by comparing second-order derivatives predicted: (a) as point values at a certain height and (b) as mean values along track with a certain sampling, at the same height (computed by numerical integration).

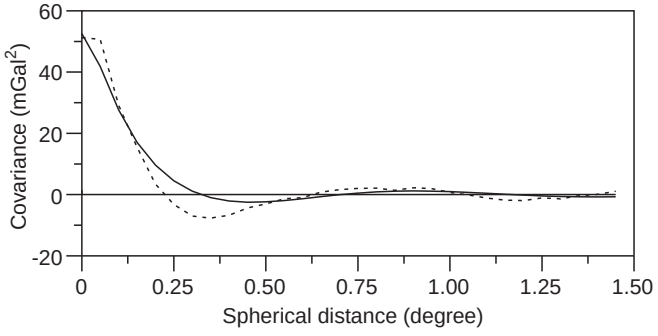

Fig. 5. Covariance function of the free-air gravity anomalies reduced to OSU91A in Canada (data set B). *Dashed line* Empirical; *solid line* analytical

Table 3. Analytically derived standard deviations of gravity and of three different types of second-order derivatives for four different altitudes (related to area B)

Altitude (km)	Gravity (mGal)	T_{zz} (EU)	$2*T_{xy}$ (EU)	T_{xx} (EU)
0	7.416	2.688	1.634	1.897
200	0.523	0.053	0.032	0.037
300	0.233	0.018	0.011	0.013
400	0.126	0.008	0.004	0.005

For this reason we predicted again T_{zz} at 200 km altitude, in the previously mentioned $15' \times 15'$ grid, as mean values along track with a data sampling corresponding to 4 s (15 arc min). Track azimuth equal to 0° was adopted in this case in order to simplify calculations. The comparison between the point and mean T_{zz} showed differences up to 0.0001 EU. These differences are considered as negligible, so that in the experiments concerning the recovery of the systematic errors we decided to use the files with the second-order derivatives predicted as point values. It should be noted that this may not be a valid procedure in areas with a more varying gravity field.

In order to study the effect of the resolution of the surface data in the upward continuation procedure, we performed four numerical experiments according to the following scheme: we used point data in a $2° \times 2°$, $3° \times 3°$, $4° \times 4°$ and $5° \times 5°$ area surrounded each time by mean $30' \times 30'$ data up to the outer bounds of the test field. In Fig. 6 the variation of the prediction error for T_{zz} along the meridian of 115° by increasing the point data collection area is shown.

The Poisson integral implemented in algorithms taking advantage of the FFT (Tscherning et al., 1994) was also used in order to create simulated gravity gradient data. For this reason, the gravity anomaly field was upward-continued to 200, 300 and 400 km altitude and subsequently these values were transformed to second-order derivative values at the corresponding altitudes. In Fig. 7 the free-air gravity anomaly field at 200 km altitude is presented, while in Fig. 8 the corresponding T_{zz} field at 200 km is shown. From Fig. 7 it is seen that the free-air gravity field is very smooth at 200 km altitude and from Fig. 8 it is evident that the T_{zz} field is strongly correlated with the free-air gravity field. Finally, in Fig. 9 the T_{zz} component at 200 km altitude computed by LSC is presented. The computed T_{zz} using FFT agree with the corresponding T_{zz} from LSC within three times the estimated error of upward continuation calculated by LSC.

4 Simulations of the recovery of systematic errors and errors of the recovered quantities

With LSC it is possible to study the recovery of systematic errors without using "data". The error

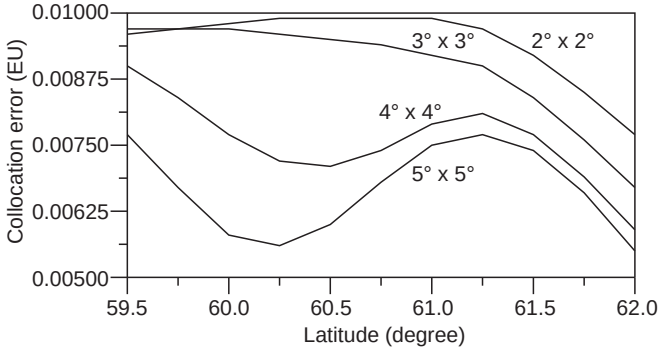

Fig. 6. Variation of the error of prediction of *Tzz* at 200 km altitude along the 115° meridian by increasing the point data collection area

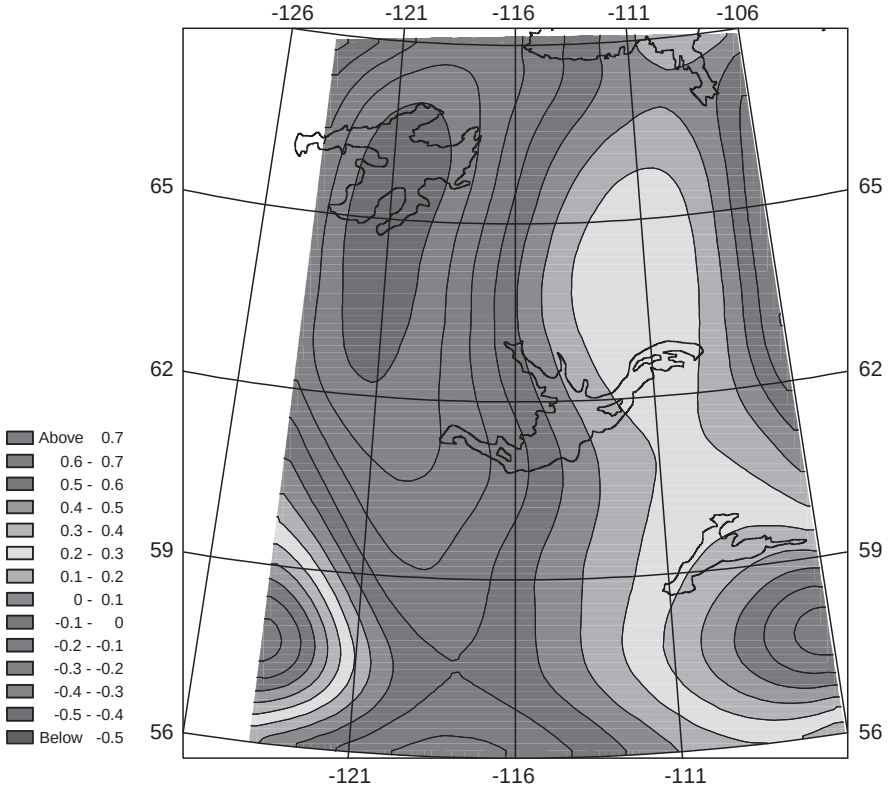

Fig. 7. Free-air gravity anomalies minus OSU91A at 200 km altitude. (mGal)

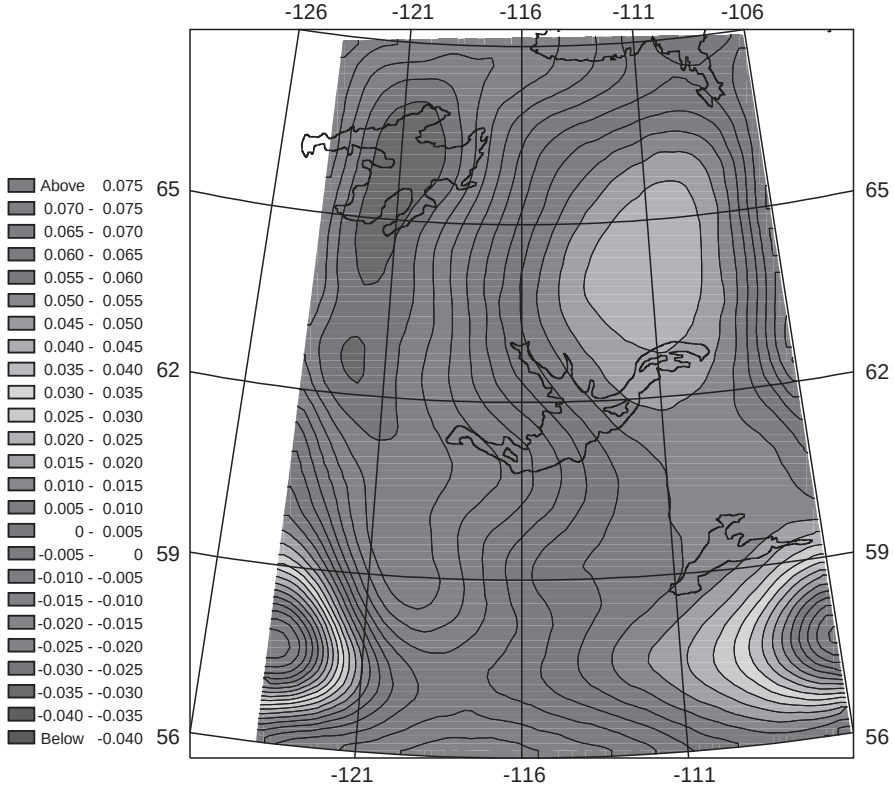

Fig. 8. *Tzz* minus OSU91A at 200 km altitude computed by FFT (EU)

estimates obtained from LSC are calculated solely from the covariances. However, we wanted to test the consistency between the error estimates and differences obtained using simulated data. Therefore new simulated data sets were produced, adding biases and tilts to the previously described simulated gravity gradients. These systematic errors were added in such a way that data lying on the same ''track'' (e.g. data with the same

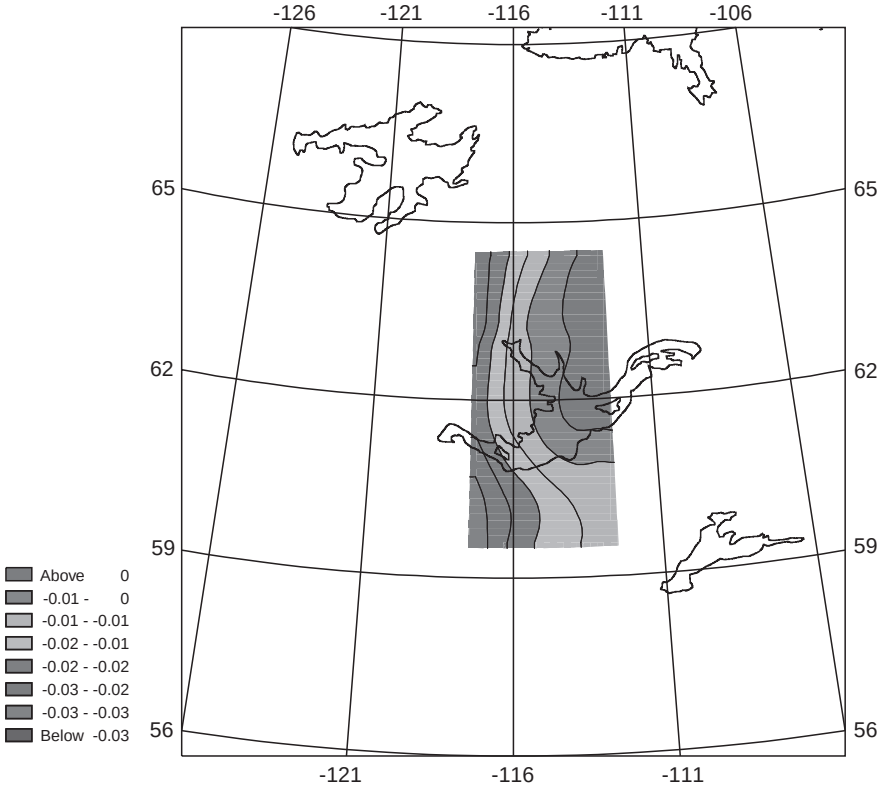

Fig. 9. Tzz – OSU91A at 200 km altitude computed by LSC (EU)

longitude) present the same bias and the same tilt. The experiments started assuming that the gradients were affected only by bias. However, in actual experiment one has to assume simultaneously bias and tilt, here we were trying to illustrate the problem step by step. In a preliminary experiment, bias was added to the T_{zz} values from data set B at 200 km. The biased T_{zz} values were used to predict ground surface point data and simultaneously to estimate the bias parameters together with the error of the estimation.

The bias parameters in this case were 21 different values (one per each track) with a priori known statistics (mean value and standard deviation equal to 0 and to 0.03 EU, respectively). However, this standard deviation is about two times larger than the standard deviation of e.g. T_{zz} at 200 km altitude (see Table 2); it should be mentioned that the values of Table 2 are reduced to OSU91A. The corresponding standard deviation of the unreduced quantities reaches 0.05879 EU, which is about two times larger than the standard deviation of the bias parameters. With this level of systematic errors we have values which are neither too small nor too large, when used to illustrate the results by examples. The comparison of the estimated with the original bias parameters showed that the estimated quantities agreed with the original ones within the error of estimation (see Table 4).

Since the collocation error estimates depends strongly on the choice of the covariance function we tried to study the effect of the accuracy adopted for the data on the results of the parameters' estimation. For this reason the previously described experiment was repeated assuming data accuracies equal to 0.01 and 0.0005 EU.

Table 4. Original and estimated bias parameters and the error of estimation. The 21 original bias parameters have an a priori mean value and SD equal to 0 and 0.03 EU, respectively. Accuracy of the T_{zz} values (collocation estimates) is equal to 0.005 EU

	Original bias parameters	Estimated bias parameters	Error of estimation
1	−0.040	−0.054061	0.005625
2	0.004	−0.009495	0.005610
3	−0.038	0.050961	0.005598
4	0.004	−0.008407	0.005589
5	0.005	−0.006811	0.005583
6	−0.069	−0.080197	0.005578
7	0.036	0.015476	0.005575
8	0.043	0.033178	0.005572
9	0.047	0.037921	0.005571
10	0.001	−0.007322	0.005570
11	−0.041	−0.048520	0.005570
12	0.015	0.008275	0.005570
13	−0.031	−0.036945	0.005571
14	0.002	−0.003139	0.005572
15	0.023	0.018646	0.005575
16	−0.026	−0.029578	0.005578
17	−0.013	−0.015828	0.005583
18	−0.052	−0.054090	0.005589
19	0.007	0.005600	0.005598
20	−0.023	−0.023749	0.005610
21	−0.043	−0.043144	0.005625

The statistics of the comparison between the original bias parameters and the corresponding estimated are summarized in Table 5, column 1.

From Table 5 it is shown that 84.5% of the standard deviation of the original bias has been recovered in the

Table 5. Statistics of the differences between original and estimated bias parameters for three different data accuracies (21 bias parameters). Mean error of the estimation is shown in parenthesis

Data accuracy	Input data (EU)			
	T_{zz}		T_{zz} + gravity anomalies	
	Mean	SD	Mean	SD
0.01	0.008260	0.004657 (0.0060)	0.000357	0.003861 (0.00433)
0.005	0.007998	0.004661 (0.0059)	0.000313	0.003880 (0.00381)
0.0005	0.007341	0.004495 (0.0056)	0.001425	0.003966 (0.00336)

simple case where no crossing tracks have been used. However, there is a bias of about 0.008 EU which should not be ignored. This bias is due to the fact that LSC utilizes norm-minimization to fix the so-called null space. The result is a bias significantly different from zero.

In theory this situation could be significantly improved by combining ground level data (e.g. gravity anomalies) with the satellite second-order derivatives (null space). This was verified in the next experiments where a set of point gravity anomalies with a resolution of 10 ft was added to the previous T_{zz} data set (see Table 5, column 2). The experiment was performed again for three different accuracy values for the T_{zz} data, while for the gravity data the value of 1 mGal was adopted for the three cases.

The lower accuracy for data accuracy equal to 0.0005 is an effect caused by numerical instabilities of the normal equations used to compute the values. The noise variance is in LSC added to the diagonal elements of the normal equations, so a high noise stabilizes the solution process. It therefore does not indicate that better results can not be obtained using other numerical procedures.

The case of using crossing ground tracks (not "crossing" at satellite altitude) is more interesting since the accuracy of the estimation of the bias parameters was significantly improved. In the following experiments, seven tracks in the direction East were to West were added to the previously described T_{zz} data set consisting of 21 tracks in the direction from South to North, so that the new data set simulated crossing satellite tracks. In this case we have 28 bias parameters chosen also to have mean value equal to 0 and SD equal to 0.03 EU. Figure 10 shows the T_{zz} field biased in this way. From this figure it is evident that a bias with SD equal to 0.03 EU causes a very strong distortion of the T_{zz} field. The results of the bias estimation (without the combination of data at ground level) in terms of the mean value and SD of the differences (original–estimated parameters) are summarized in Table 6, column 1.

However, the uncertainty in the mean is almost the same as in the case of Table 5 (column 1) but there the SD has been considerably decreased.

When surface gravity anomalies are combined with the T_{zz} data set there is a significant improvement in the mean uncertainty, as it is shown in Table 6, column 2. In addition, the increase in the corresponding SD after the combination of T_{zz} with gravity data is due to the lack of

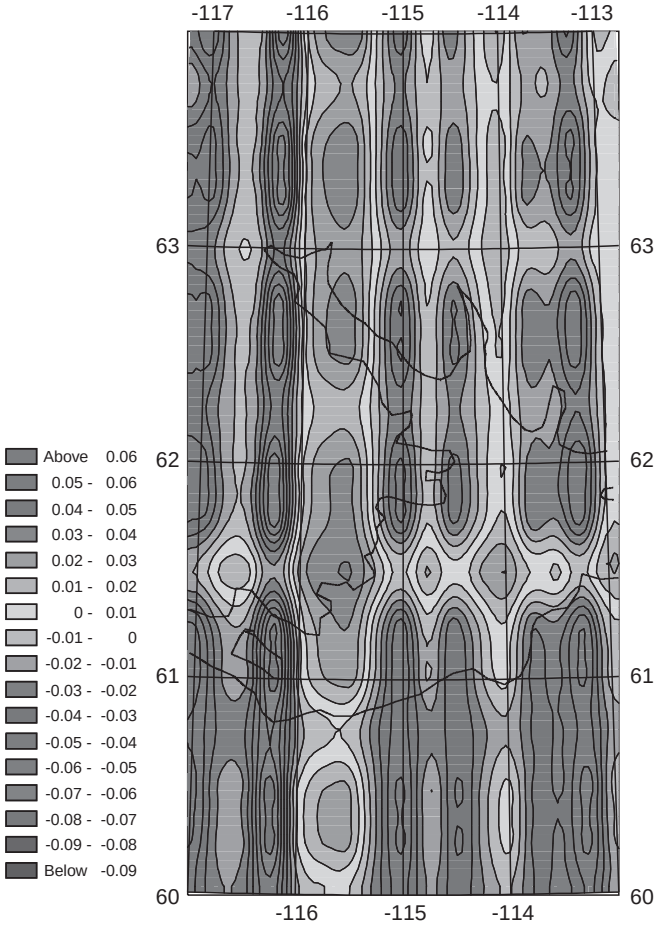

Fig. 10. *Tzz* – OSU91A at 200 km altitude artificially biased (EU)

the stabilizing effect. Nevertheless, the results of Table 6 are significantly better than those of Table 5, at least in terms of standard deviation of the differences between observed and estimated bias parameters.

Another sequence of experiments was carried out where the bias parameters from T_{zz} (data set B) at altitudes of 300 and 400 km were estimated. The experiments were performed for the cases of (a) crossing tracks (28 parameters) and (b) the combination of crossing tracks with surface gravity anomalies. In these experiments the a priori standard deviation of the bias parameters in 300 km altitude was set equal to 0.01 EU and for 400 km 0.005 EU. For the T_{zz} data an accuracy equal to 0.002 and 0.001 EU was adopted for 300 and 400 km,

Table 6. Statistics of the comparison of the estimated bias with the original in the case of crossing tracks. Number of parameters is 28 with mean value 0 and SD 0.03 EU. Mean error of the estimation is shown in parenthesis

Data accuracy	Input data (EU)			
	T_{zz}		T_{zz} + gravity anomalies	
	Mean	SD	Mean	SD
0.01	0.007403	0.000369 (0.00485)	0.000105	0.000794 (0.00393)
0.005	0.006982	0.000182 (0.00412)	−0.000138	0.000371 (0.00342)
0.0005	0.007188	0.000024 (0.00332)	0.001478	0.000026 (0.00298)

Table 7. Statistics of the differences (EU) between original and estimated bias parameters from crossing tracks of T_{zz} at 300 and 400 km, respectively. Mean error of the collocation estimation is given in parenthesis

Height (km)	Input data (EU)			
	T_{zz}		T_{zz} + gravity anomalies	
	Mean	SD	Mean	SD
300	0.005320	0.000097 (0.0001942)	0.002903	0.000192 (0.0001729)
400	0.003697	0.000051 (0.001071)	0.002960	0.000086 (0.001025)

respectively. These values are the collocation error estimates of the prediction of T_{zz} from gravity anomalies. The results of these experiments are shown in Table 7.

In order to study the possibility of recovering the bias parameters in the case of a lower signal-to-noise ratio, we have use biased T_{zz} from the data set A in order to estimate the bias parameters. In the experiment the a priori standard deviation of the bias parameters was equal to 0.03 EU and the bias was estimated from (a) T_{zz} (crossing tracks, 28 parameters) only and (b) from combination of T_{zz} (crossing tracks) with surface gravity anomalies. The results from these experiments are summarized in Table 8.

Comparing the results of Table 8 (column 1) with the corresponding results of Table 6 (column 2, row 2), we see that in the case of data set A these are slightly better than the corresponding from data set B. Comparing the results of Table 8, column 2, with the corresponding results of Table 6 (column 2, row 2), we see that the T_{zz} from data set B gives a better mean value of differences, but T_{zz} from A gives better standard deviation, so that from the results of the last experiments it is not possible to draw a conclusion.

In order to study the possibility of estimating a very small bias, e.g. of the order of 2–3% of the standard deviation of the corresponding data in the corresponding altitude, we performed experiments using T_{zz} from data set A and bias with an a priori SD equal to 0.0005 EU. The results from these experiments are shown in Table 9.

From Table 9 it is also evident that a very small bias can be detected especially in the case of combining surface gravity anomalies with the second-order derivatives at satellite altitude.

Finally, the T_{xz} values from data set B at 200 km have been used in order to estimate the bias parameters. The results of this estimation are shown in Table 10.

Table 8. Statistics of the differences (EU) between original and estimated bias parameters from T_{zz} (data set A) at 200 km crossing tracks (28 parameters) and from a combination of T_{zz} with surface gravity anomalies. The a priori standard deviation of the bias parameters was equal to 0.03 EU. For T_{zz} data an accuracy equal to 0.005 EU was adopted. Mean error of the collocation estimation is given in parenthesis

	T_{zz}	T_{zz} + gravity anomalies
Mean	0.005363	−0.000857
SD	0.000138 (0.0004118)	0.000269 (0.003011)

Table 9. Statistics of the differences (EU) between original and estimated bias parameters from T_{zz} (data set A) at 200 km crossing tracks (28 parameters) and from a combination of T_{zz} with surface gravity anomalies. The a priori standard deviation of the bias parameters was equal to 0.0005 EU. For T_{zz} data an accuracy equal to 0.005 EU was adopted. Mean error of the collocation estimation is given in parenthesis

	T_{zz}	T_{zz} + gravity anomalies
Mean	0.005045	0.000039
SD	0.000043 (0.003619)	0.000056 (0.002511)

Table 10. Statistics of the differences (EU) (original – estimated) bias parameters from T_{xz} (data set B) at 200 km crossing tracks (28 parameters) and from a combination of T_{xz} with surface gravity anomalies. The a priori standard deviation of the bias parameters was equal to 0.03 EU. For T_{zz} data an accuracy equal to 0.003 EU was adopted. Mean error of the collocation estimation is given in parenthesis

	T_{xz}	T_{xz} + gravity anomalies
Mean	−0.007924	−0.007628
SD	0.000125 (0.002466)	0.000186 (0.002451)

Table 11. Statistics of the differences between original and estimated bias and tilt parameters from T_{zz} (data set B) at 200 km (28 parameters for bias and 28 for tilt), alone or in combination with surface gravity data. The a priori standard deviation of the bias parameters was equal to 0.003 EU and that of the tilt equal to 0.003 EU/100 km. For the T_{zz} data an accuracy equal to 0.005 EU was adopted. Mean error of the collocation estimation is given in parenthesis

	Bias (EU)		Tilt (EU/100 km)	
	Mean	SD	Mean	SD
Crossing tracks	−0.007050	0.005778 (0.008205)	−0.000014	0.000397 (0.000652)
Crossing tracks + gravity anomalies	−0.000178	0.005679 (0.006630)	0.000014	0.000394 (0.000559)

Considering the results of Table 10, we see that the bias remains almost the same even after the combination of surface gravity anomalies. Concerning the standard deviation of the differences (observed − predicted), the situation is very similar to the corresponding one when using the T_{zz} values for the bias estimation.

The experiments for the estimation of systematic errors were completed by investigating the case where the data are affected simultaneously by bias and tilt, since this is the realistic situation. For this reason tilt was artificially added to the already biased predicted second-order derivatives, used in the previous experiments for the recovery of the bias parameters. The tilt added presents a mean value equal to 0 EU and a SD equal to 0.003 EU/100 km. This value was selected based on the observation that the total length of the simulated tracks in the North–South direction is about 555 km, so the SD of the tilt of a track from North to South is about 0.017 EU, i.e. equal to the SD of the T_{zz} values (data set A) at 200 km altitude. The results summarized in Table 11 concern the bias and tilt estimation in the case of (a) T_{zz} crossing tracks, and (b) T_{zz} crossing tracks combined with surface gravity anomalies.

From the results of Table 11 we see that the standard deviation of the differences between original and estimated bias and tilt agree with the corresponding mean error estimate from collocation. As in the earlier results, this is only showing that the actual software implementation (GEOCOL) works correctly.

5 Conclusion

The described simulations showed that the recovery of bias parameters from second-order derivative SGG "measurements" is possible with an accuracy down to 50% of the random data noise. The use of crossing tracks helps to improve the bias estimation.

The mean value of the differences (original − estimated bias parameters) obtained from simulated data is relatively large compared to the standard deviation of the corresponding second-order derivative component at the corresponding height. This mean value almost vanishes when gravity data at ground level are combined with the second-order derivative data set. This shows the usefulness of combining space data with ground data.

In the case of simultaneous estimation of bias and tilt parameters from T_{zz} "measurements", the collocation error estimates are double the error estimates obtained when the observations are only supposed to be contaminated by a bias noise. However, this error is still at the level of the supposed random data noise. This verifies that such errors can be consistently removed.

Acknowledgements. Thanks are due to R. Forsberg (National Survey & Cadastre, Denmark) for providing gravity data and to R.H. Rapp (Columbus, Ohio) for the OSU91A model. This paper has been carried out in the framework of a project supported by ESA/ESTEC contract JP/95-4-137/MS/NR.

References

Knudsen P (1987) Estimation and modelling of the local empirical covariance function using gravity and satellite altimeter data. Bull Geod 61: 145–160

Moritz H (1980) Advanced physical geodesy. H. Wichmann, Karlsruhe

Rapp RH, Pavlis NK (1990) The development of geopotential coefficient models to spherical harmonic degree 360. J Geophys Res 95: 21885–21911

Schwarz KP, Sideris MG, Forsberg R (1990) The use of FFT techniques in physical geodesy. Geophys J Int 100: 485–514

Tscherning CC (1995) GEOCOL – a FORTRAN program for gravity field approximation by collocation, 11th edn. Technical note, Geophysical Institute, University of Copenhagen

Tscherning CC, Knudsen P, Forsberg R (1994) Description of the GRAVSOFT package, 4th edn. Technical report, Geophysical Institute, University of Copenhagen